ABSTRACT

*Nonwoven webs are widely used as filters, and their use is rapidly increasing every year. Charging the fibers in the nonwoven webs can greatly improve their filtration efficiency by increasing the capture of small particles traveling at low velocity. This paper describes the mechanisms of corona charging of nonwoven webs. Different charging techniques for producing melt-blown electrets are also discussed.*

**Application:**

*Describes useful electrode configurations for imparting electret properties to melt-blown webs.*

# Theory and techniques of electrostatic charging of melt-blown nonwoven webs

PETER PING-YI TSAI, GUO-WEI QIN, AND LARRY C. WADSWORTH

An electret, a counterpart to a magnet, is a dielectric material that exhibits a permanent electric field or stores permanent charges without requiring an externally applied voltage. Electrets have a large variety of applications, including transducers, generators, air filters, etc. *(1)*. Electrets are made by either polarizing or electrostatically charging a dielectric material.

Charging mechanisms for nonwoven webs have been described in an earlier work *(2)*. This paper describes the theory of corona charging and the charging techniques that can be used at various locations on melt-blowing lines.

Melt blowing is a one-step process for manufacturing nonwoven webs directly from polymeric resin *(3)*. Melt-blown webs are ideally suited as filters because their ultrafine fibers provide high surface area, thereby increasing the probability of particle entrapment by mechanical forces. Nevertheless, even greater filtration efficiency can be achieved by introducing electrostatic charges into fibers to attract the filtered particles by electric forces.

## THEORY OF ELECTRICAL DISCHARGES IN THE AIR

### General

A portion of the air ($10^9$ molecules out of $10^{25}$ molecules/m$^3$ at sea level) is ionized by cosmic rays and by radiation of radioactive bodies. Different gases have different ionization potentials at different pressures. For example, dry air is ionized by an electric field of 30 kV/cm at 1 atm pressure and by a field of 10 kV/cm at low pressure. Dark, glow, and arc discharges are three regimes of electrical discharge through air ionization by electric field *(4)*. Corona discharge in the dark-discharge regime is used for electrostatically charging dielectric materials to make an electret. In air at 1 atm pressure, glow discharge may not occur, but arcing occurs when voltage is raised to obtain a high corona-discharge current. High voltage, but low current, is required for corona generation. Hence voltage in the power supply is limited by a low current output. Voltage in the power supply drops whenever an arcing (a high current-density discharge) occurs. Nevertheless, several electrode configurations have been developed to generate sufficient corona-discharge current before arcing occurs.

This paper describes some useful electrode configurations along with their electric field distributions. The electric field distributions are important for determining electrode dimensions, the gap between the electrodes, and the voltage to be applied to the electrodes. For corona discharge, the electric field should be higher than the air ionization potential but lower than the arcing potential between the electrodes.

### Electrode configurations

***Configuration 1.*** Configuration 1 is a biased sharp point or wire above a grounded plate, as shown in **Fig. 1**. The surface electric field ($E_s$) of the sharp point or wire above the grounded plate can be approximated (4) as

$$E_s = (V_0/a)\ \{1/[1-(a/b)]\} \qquad (1)$$

and the radial electric field, $E(r)$, of the sharp point or wire can be approximated as

$$E(r) = (V_0 a/r^2)\ \{1/[1-(a/b)]\} \qquad (2)$$

where

| | | |
|---|---|---|
| $V_0$ | = | applied voltage |
| $a$ | = | radius of the sharp point or wire |
| $b$ | = | distance from the sharp point or wire to the plate |
| $r$ | = | radial distance from the sharp point or wire |

***Configuration 2.*** Configuration 2 is a biased wire in the center of a grounded shell, as shown in **Fig. 2**. The surface electric field along the wire is

$$E_s = V_0/[a \ln(b/a)] \qquad (3)$$

and the radial electric field of the wire is

$$E(r) = V_0/[r \ln(b/a)] \qquad (4)$$

where

| | | |
|---|---|---|
| $a$ | = | radius of the wire |
| $b$ | = | radius of the shell |
| $r$ | = | radial distance. |

***Configuration 3.*** Configuration 3 is a biased wire or a wire grid between two parallel plates, as shown in **Fig. 3**. The surface electric field of a biased wire between two parallel plates is

$$E_s = V_0/[a \ln(4b/\check{s}a)] \quad (5)$$

and the surface electric field of a wire grid between two parallel plates is *(5)*

$$E_s = V_0/a\Big[[\ln(4b/\check{s}a)] + \sum_{k=1}^{n} \ln\Big(\cosh\{[(k\check{s}/2)(d/b)]+1\}/\cosh\{[(k\check{s}/2)(d/b)]-1\}\Big)\Big] \quad (6)$$

where

| | | |
|---|---|---|
| $a$ | = | radius of the wire |
| $b$ | = | distance from the wire center to the plate |
| $d$ | = | distance between two wires |
| $n$ | = | number of wires. |

***Configuration 4.*** Configuration 4 is a biased wire parallel to a grounded wire, as shown in **Fig. 4**. The surface electric field along the biased wire is

$$E_s = V_0/a\Big[[(s-2a)/(s+2a)]^{1/2} + \ln\Big((s/2a)+\{[s^2/(2a)^2]-1\}^{1/2}\Big)\Big] \quad (7)$$

If $s>a$, the surface electric field is reduced to

$$E_s = V_0/[a \ln(s/a)] \quad (8)$$

where

| | | |
|---|---|---|
| $a$ | = | radius of the wire |
| $s$ | = | distance between the two wires. |

### *Application of electrostatic charge*

The previous equations are used to calculate the intensity of the electric field for the various electrode configurations. Once the field intensity is known, the air ionization and the particle motion between the electrodes can be understood. These are important considerations in applying electrostatic charges to the melt-blown fibers in electret filters, since the charges are applied to maximize filtration efficiency at given pressure drops.

The regime in which the electric field is higher than the air breakdown potential, i.e., 30 kV/cm for dry air at 1 atm pressure, is called the active volume, and the radius is called the active radius. When a neutral air molecule breaks down in the active region of a positively biased electrode, a positive ion and an electron are formed. The positive ion is repelled toward the grounded electrode by the positive electrode. The electron (a) attaches to electronegative molecules, such as nitrogen and oxygen, to form a negative ion in a time frame of less than 1 ms, or (b) ejects another electron from a neutral molecule or an ion, depending on the electron kinetic energy. Finally, the electron and the negative ion are attracted to the positive electrode, and the isolated electron or the electron(s) from the negative ion is drawn by the positive electrode and a neutral molecule is released. The drawn electrons pass through the power supply and form the power supply current. The opposite phenomenon is true for a negative electrode.

Field charging is accomplished when the filter material passes between the two electrodes in which charges are moving from one electrode to the other by the electric field force. If a material is not charged between two electrodes under the electric force action, an extra force such as aerodynamic force is needed to accomplish the charging. Charging by the latter case is no longer called field charging, but, rather, remote charging.

Suppose that the sharp point or the wire radius for Configuration 1 is 0.2 mm and that the gap between the sharp point and the grounded plate (or between the wire and the grounded plate) is 5 cm. Then the electric field (expressed in units of V/m) on the surface of the sharp point or the wire is

$$E_s = [V_0/(0.2 \times 10^{-3})]\ \{1/[1-(0.02/5)]\} = 5.02 \times 10^3\ V_0$$

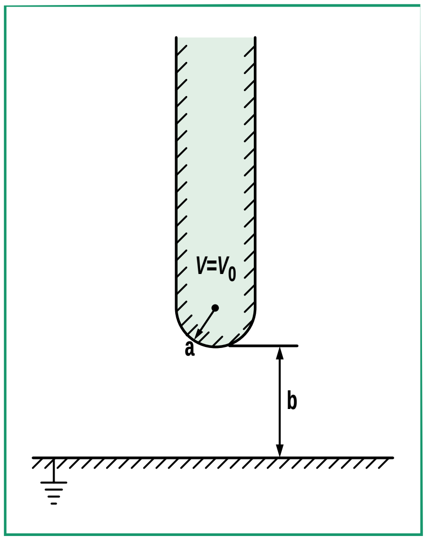


***1. Corona discharge around a biased sharp point above a grounded plate***

The electric field to break down the air is about 3 MV/m. So, the minimum applied voltage, Vô, is 600 V. The electrode surface ionization, however, does not provide enough corona charges for effective electrical charging. To obtain effective charging, the voltage should be much higher than that required to ionize the electrode surface, as long as the arcing voltage is not exceeded.

Actually, the electric field must be higher than the breakdown electric field for air if the objective is to initiate coronal discharge. For example, the initiating electric field for the pin above the grounded plate (**Fig. 1**) is *(6)*

$$E_{sc} = 1.8 \times 10^5/a^{1/2} \quad (9)$$

where

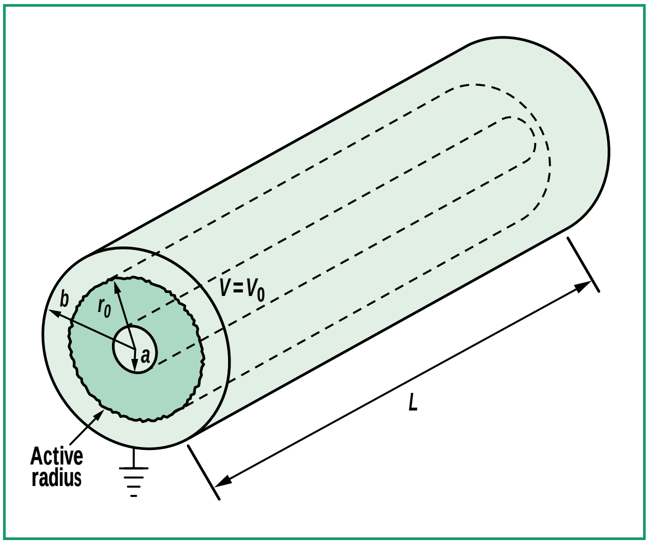


2. Corona discharge around a biased wire within a grounded shell

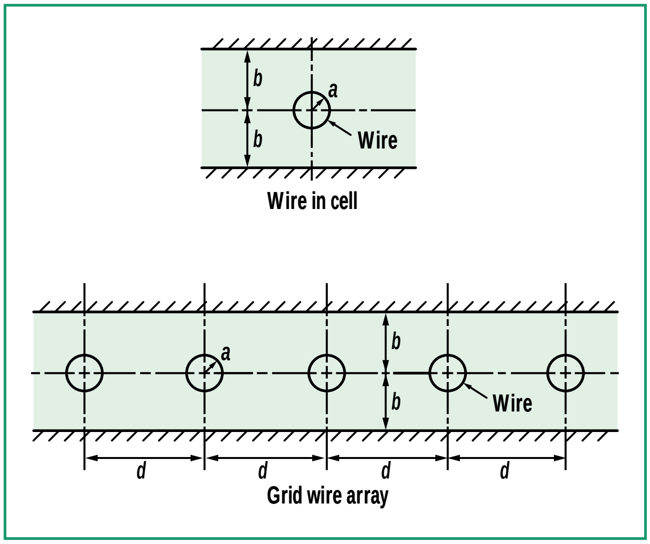


3. Corona discharge around a biased wire and a biased wire grid between two parallel plates

$E_{sc}$ = initiating electric field

The initiating electrical field for a wire with a radius of 0.2 mm in this configuration is $E_{sc}$ = 12.73 x $10^6$ V/m, which is much greater than the breakdown electric field of the air (3 x $10^6$ V/m).

Despite the effect of electrode configuration on the air discharges, there are other factors—the roughness of the wire, air pressure, thermal temperature, etc.—that exert a significant effect on the magnitude of the electric field intensity that ionizes the air. For example, the coronal onset electric field for a wire between two grounded parallel plates is *(7)*

$$E_c = (0.6)(3.126 \times 10^6)[d_r + 0.0301(d_r/r_w)^{1/2}] \quad (10)$$

where

$E_c$ = coronal onset field, V/m
$d_r$ = relative gas density, referred to 1 atm pressure at 20°C
$r_w$ = radius of the wire, m
0.6 = correction factor for wire roughness.

The electric field generated by the applied voltage will be distorted by the discharges in the air. Equation 11 shows the effect of the discharges on the electric field for Configuration 2.

$$E(r) = (1/r)\{(a^2 E_s^2) + [(I_c a^2 - I_c r^2)/2\text{š}L\mu_i[\varepsilon]_0]\}^{1/2} \quad (11)$$

where

$I_c$ = discharge current
$L$ = inductance
$\mu_i$ = ion mobility
$[\varepsilon]_0$ = permittivity in vacuum.

Note that Eq. 11 becomes Eq. 4 if the effect of discharges on the electric field distribution is not considered. The electric field distribution between the electrodes is complicated, depending on the electrode configuration, air content, air pressure and temperature, the air discharge concentration, etc. Experimentation is usually required to determine the parameters needed to obtain a high charging efficiency on the nonwoven webs. Some useful charging techniques for melt-blown webs are described in the next section.

## TECHNIQUES FOR APPLYING ELECTROSTATIC CHARGES TO MELT-BLOWN WEBS

Numerous techniques have been patented for electrostatically charging melt-blown webs. Several patents have been issued in which electrostatic charging is accomplished at different steps of the melt-blowing process. The various positions are identified in **Fig. 5**.

A patent by Deeds *(8)* (assigned to Exxon Chemical Co.) uses corona wires in the upper and lower primary hot-air plenums near the air exit region (position A in **Fig. 5**). The electrode configuration is shown in **Fig. 3** (Configuration 3). Corona charges are generated around a biased wire in two parallel plates in the air path, and the charges are forced to move out of the air path by the air stream that is used to attenuate the fibers. The charges are embedded into molten fibers near the die tip purely by aerodynamic force from the air stream.

KEYWORDS
*Nonwovens, webs, theories, melt blowing, filters, corona discharge, electrostatic charge, filtration, efficiency, techniques.*

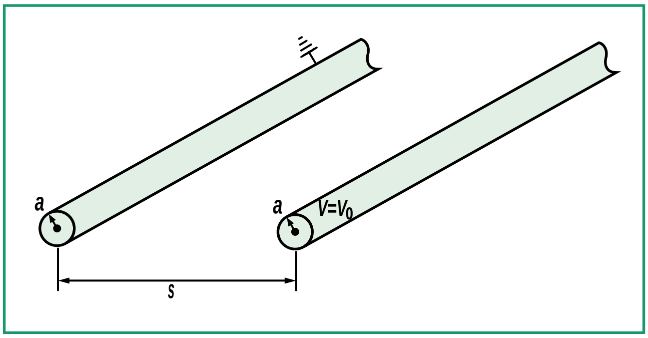


*4. Corona discharge around a biased wire parallel to a grounded wire*

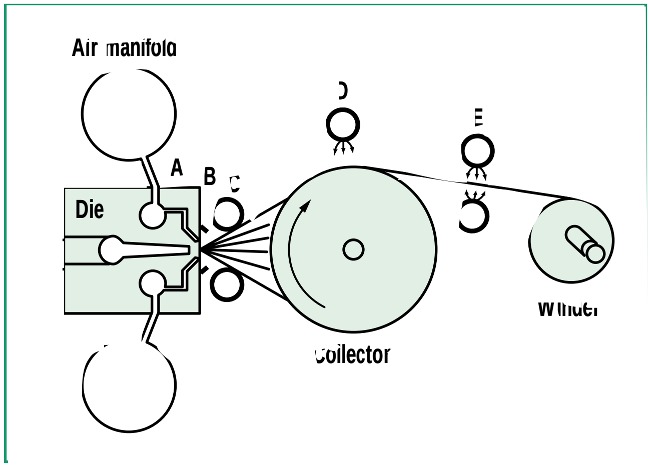


*5. Charging locations in melt-blowing line*

A patent by Moosmayer *et al.* *(9)* (assigned to Exxon Chemical Co.) uses two rows of corona pins above and below the row of spinneret holes and air slots (positions B and C in **Fig. 5**). The electrode configuration is illustrated in **Fig. 1** (Configuration 1). Charges are generated by the pins attached to the air-knife plate, and they are moved by electric field force to the biased bar electrodes located 2–8 cm from the corona pins and about 5 cm apart. The charges can be moved out of the electric field lines by the aerodynamic force. Charges are embedded into the molten fibers by field force and/or by aerodynamic force.

A patent issued to Kubik *et al.* of 3M *(10)* involves a technique that uses electrode Configuration 2 (**Fig. 2**). The electrode is located at position C in **Fig. 5**. Corona charges are generated around the biased wire in the shell. There is no electric field across the fiber path because both wires—one on the top of the fiber path and the other on the bottom—are simultaneously biased either positive or negative voltage. Charges are embedded into the molten fibers by aerodynamic force.

Patents issued to Nakao *(11)* and Togashi *et al.* *(12)* are based on electrode Configuration 1 (**Fig. 1**). A wire (or several wires) or a row (or several rows) of pins are arranged above a grounded drum (position D in **Fig. 5**). Corona charges are generated around the biased pin points or along the biased wires. Charges are embedded into the fibers in the fabric by the electric field force formed between the biased pins or wire(s) and the grounded drum that the fabric passes over.

Patents issued to Wadsworth *et al.* *(13)* and Klaase *et al.* *(14)* are based on electrode Configuration 4 (**Fig. 4**). The electrode is located at position E in **Fig. 5**. These inventions involve the use of two wires or two row of pins arranged in parallel. Charges are generated at both the two wires or the two rows of pins. The charges are embedded into the fibers in the fabric by the electric field force created between the two electrodes through the use of semiconductive material in contact with the melt-blown web.

The charging techniques located near the die outlet—positions A, B, and C in **Fig. 5**—are directed toward charging fibers, while charging techniques farther downstream—at positions D and E—are performed on fabric. The effects on charging are different for the two cases. In the first case, fibers are either in molten form or are still hot. In the second case, the fibers are solidified or cooled to a low temperature and the fibers are compacted to form the web. Charges applied near the die outlet can migrate before the fibers are solidified, but charging will not be affected by the thickness of the web. On the other hand, charges applied farther downstream to the web may not migrate in the fibers, but the effectiveness of the charge can be influenced by the web thickness.

A new charging technique patented by Tsai and Wadsworth *(15)* (assigned to the University of Tennessee) comprises two electrode configurations, similar to Configurations 1 and 2, which can efficiently charge thin and thick nonwoven webs, respectively, at location E in **Fig. 5** or off the melt-blown line.

## CONCLUSION

Two mechanisms are involved in producing nonwoven electrets.

1. Generation of charges through air ionization by electric field intensity
2. Embedment of charges into molten fibers or solidified fibers in the fabric through contact media by aerodynamic force and/or by electric field that ionizes the air.

Numerous patents have been issued based on this simple process. Work is underway to improve the charging and filtration efficiencies of filters. TJ

*Tsai is a research professor and Wadsworth is a professor and director of the Textiles & Nonwovens Development Center (TANDEC) at the University of Tennessee, Knoxville, TN 37996-1950. Qin is the technical manager of Tex-Tenn Corp., Gray, TN 37615.*

*The authors extend their thanks to J. Reece Roth, the author of* Industrial Plasma Engineering, *for his time in discussing the electric field distribution of different electrode configurations. His contribution of the original figures of the electrode configurations is also greatly appreciated.*

*Received for review April 10, 1995.*

*Accepted Dec. 8, 1996.*

LITERATURE CITED

1. Sessler, G. M., Electrets, Springer–Verlag, Berlin, Heidelberg, New York, 1980, p. 347.
2. Tsai, P. P. and Wadsworth, L. C., TAPPI 1994 Nonwovens Conference Proceedings, TAPPI PRESS, Atlanta, pp. 9–11.
3. Tsai, P. P. and Wadsworth, L. C., "Effect of process conditions on melt blown web properties," submitted for review by Tappi Journal.
4. Roth, J. R., Industrial Plasma Engineering, Vol. 1: Principles, Institute of Physics Publishing, Bristol and Philadelphia, 1995.
5. Bohm, J., Electrostatic Precipitators, Elsevier, North-Holland, Amsterdam, 1982.
6. Cobine, J. D., Gaseous Conductors, Dover, New York, 1958.
7. White, H. J., Industrial Electrostatic Precipitator, Addison–Wesley, Reading, MA, 1963.
8. Deeds, W. E., U.S. pat. 5,122,048 (June 16, 1992).
9. Moosmayer, P., Budliger, J., Zurcher, E., et al., U.S. pat. 4,904,174 (Feb. 27, 1990).
10. Kubik, D. A. and Davis, C. I., U.S. pat. 4,215,682 (Aug. 5, 1980).
11. Nakao, F., U.S. pat. 4,592,815 (June 3, 1986).
12. Togashi, R., and Ando, K., et al., U.S. pat. 5,051,159 (Sept. 24, 1991).
13. Wadsworth, L. W. and Hersh, S. P., U.S. pat. 4,375,718 (March 8, 1983).
14. Klaase, P.T.A., and Turnhout, J., et al., U.S. pat. 4,588,537 (May 13, 1986).
15. Tsai, P. P. and Wadsworth, L. C., U.S. pat. 5,401,446 (March 28, 1995).